

Advances in the Multi-elemental Analysis of Solder by ETV-ICPOES for the Discrimination of Forensic Evidence

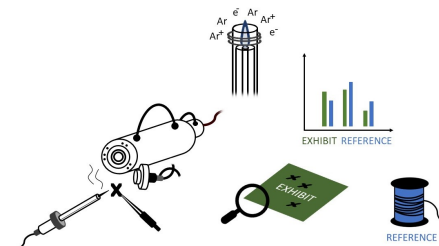
Kate Moghadam, Chloe Wheeler, and Diane Beauchemin*

Department of Chemistry, Queen's University, Kingston, ON, K7L 3N6, Canada

Received: May 18, 2023; Revised: June 29, 2023; Accepted: July 03, 2023; Available online: July 04, 2023.

DOI: 10.46770/AS.2023.113

ABSTRACT: Lead-tin solder is a useful piece of evidence from a crime scene and may be examined for information related to the construction or source of an improvised explosive device (IED). A technique based on electrothermal vaporization into inductively coupled plasma optical emission spectrometry was improved for the direct quantification of trace and major elements in solder (Ag, As, Bi, Cr, Fe, Sb, Sn). NIST 1728, a tin-alloy certified reference material, was used for external calibration and achieve a direct, fully solid-sampling procedure using only 0.5–3.0 mg of sample. Point-by-point internal standardization with Ar 404.442 nm was performed to compensate for sample loading effects on the plasma, and a background correction technique was introduced to improve the overall efficiency of analysis. As solder was observed to change composition during some mock scenarios of IED preparation, which limits how solder can be examined in forensics, different soldering conditions (temperature, solder size, cleaning of the soldering tip or not between subsequent samples) were studied using an Fe-tip soldering device. Statistical analyses including Student's t-tests and a one-way analysis of variance revealed that none of these conditions resulted in contamination of the melted solder sample, hence confirming the viability of the mock procedure used to replicate IED soldering in research. A new qualitative discrimination method is introduced and demonstrated in a blind trial for matching and discriminating lead-tin solders. This method represents an improvement from past research and has potential for use in evaluating other forensic evidence involving ferrous-alloys.



INTRODUCTION

Improvised explosive devices (IEDs), colloquially known as “homemade bombs”, form a broad category of crude yet sophisticated weapons systems that are designed to “destroy, incapacitate, harass, or distract”.¹ The design systems of IEDs are highly variable and may be modified depending on the destructive impact or intended campaign target; however, one identified commonality in these design systems is solder.^{2,3} Lead-tin solder is a fusible metal alloy used to bond workpieces in an electrical circuit. Most lead-tin solders contain a rosin core to aid with melting and solder wetting (*i.e.*, adherence to other metal surfaces),⁴ providing an attractive option for reliable electric sequencing in the initiation or detonation of an explosive device.

Lead-tin solder has been identified as a promising piece of

physical evidence from a crime. A variety of trace impurities exist in solders because of: (1) individual manufacturer preferences for solder, and/or (2) the absence of control regulations in the manufacturing process.^{2,3} As a result, solder may be accurately distinguished and implied in crime; if solder salvaged from a crime scene is compared to solder from a suspect, a match between elemental fingerprints may identify a guilty party. This possibility has been harnessed by researchers who have discriminated solders, and successfully matched solders, on trace and major element concentrations (Bi, Cu, Sb, Ni, Pb, and Sn).^{2,3,5}

Solder analysis as a forensic technique has gained momentum in the past five years since the discovery that rosin may facilitate the contamination of elements from the soldering gun to the solder (during the melting process, “soldering”). After melting solders with a Cu-tip soldering gun, a melted portion exhibited higher

Table 1. Operating conditions for ETV-ICPOES, based on optimized conditions from Scheffler *et al.*²⁰

Parameter	Value	
ICPOES		
Radio-frequency power (KW)	1.70	
Ar plasma gas flow rate (L min ⁻¹)	14.5	
Ar auxiliary gas flow rate (L min ⁻¹)	1.50	
Plasma view	Lateral	
Signal scan mode	Transient	
Integration time (ms)	10	
Sampling rate (Hz)	10	
Observation height (mm)	10	
ETV		
Ar bypass gas flow rate (L min ⁻¹)	0.5	
Ar carrier gas flow rate (L min ⁻¹)	0.15	
CF ₄ reaction gas flow rate (mL min ⁻¹)	8.00	
Step	Temperature (°C)	Duration (s)
Temperature program for graphite boat cleaning		
Initial temperature	20	1
Cleaning	2300	45
Cooling	20	15
Temperature program for sample analysis		
Initial temperature	20	15
Pyrolysis	400	20
Cooling	20	15
Vaporization	2300	30
Cooling	20	20

concentrations of Cu than its equivalent, unmelted pair.^{3,5} This implicates the type of soldering gun (*i.e.*, type of soldering tip) used in the creation of an IED, and more importantly would correctly match solder samples on the basis of the contaminated element. This prevents the occurrence of a *false negative* where a melted solder (*i.e.*, solder salvaged from a crime) is incorrectly discriminated from its unmelted pair (*i.e.*, solder from a suspect's possession).

This possibility for melting to distort the elemental fingerprint of solder, and thus the efficacy of sample matching, warrants additional investigation into the contamination process. To date, contamination by melting has been replicated in limited settings and under fixed variable conditions; current method designs involved melting with a constant soldering gun temperature and sample size.^{3,5} There is also limited work on the effects of other solder tips, namely tips with Fe-plating. In a study using an Fe-Al-based tip for sample melting, only Cu, As, Ag, Sb, and Bi were measured in the samples, rather than the major tip elements (Al or Fe).² It is therefore inconclusive whether the major elements from other soldering tips exhibit the same pattern of contamination in rosin-solders. This is an important avenue to explore as Fe-plated tips are popular given their added durability and balance of mechanical and thermal properties.⁶ These tips contain a plated layer of Fe at the working surface, with additional layers of Cr as extra protection against corrosion.⁷ This literature inspires the current research interests: expand the elemental profile (Fe, Cr) to investigate contamination of the major tip elements from an Fe-

plated soldering tip, and identify if this contamination varies under broad user conditions including soldering gun temperature and solder sample size.

In addition, this research will investigate the impact of cleaning the solder tip during sample melting. In past research designs, reiterative cleaning of the soldering tip was done between melting samples, either by wiping with 10% HNO₃ (v/v)⁵ or by sanding, soaking in 10% (v/v) HNO₃ acid bath, and further wiping with doubly deionized water (DDW).³ There are two problems with tip cleaning. Firstly, an individual producing an IED is unlikely to employ routine cleaning measures. Secondly, trace metals (such as Fe) can be easily etched and soluble in acid and acid mixtures; several applications of etching with dilute HNO₃ have been done.⁸ Cleaning with acid may (1) etch the surface of the soldering tip, thus preventing contamination to a sample during melting, or (2) remove trace metal residue leftover from previous solder sample melts, preventing contamination from one solder sample to another. These reasons may explain why no significant increases in other elements beyond Cu were observed after melting.⁵ This introduces the final goal of the research: investigate the significance of tip cleaning and improve the mock procedure for IED soldering.

This research will use electrothermal vaporization (ETV) for sample introduction into inductively coupled plasma optical emission spectrometry (ICPOES) for multi-elemental analysis, which has been applied in numerous forensic,^{5,9-11} archaeological,¹² and environmental applications.¹³⁻¹⁸ These applications share a short analysis time, up to 85 s per sample, and study materials, artifacts, and/or evidence that is limited in mass (0.1–5 mg). In each application, an optimized temperature program is configured to resistively vaporize a sample up to 2700–2800°C. ETV replaces the need for sample digestion, which has been a reported cause of interference and analyte precipitation in past determinations of solder.³ Additional coupling to Ar-based ICPOES allows for the passive measurement of up to 70 elements with sub-parts-per-billion detection limits.¹⁹ As a result, ETV-ICPOES offers an effective approach for a direct, sensitive and robust trace element analysis.

EXPERIMENTAL

Instrumentation and operating conditions. Research was conducted using an ARCOS inductively coupled plasma optical emission spectrometer (SPECTRO Analytical Instruments, Kleve, Germany). An electrothermal vaporization system (ETV 4000C, Spectral Systems, Furstenfeldbruck, Germany) was coupled in sequence to enable direct solid sample introduction. The operating conditions for ETV-ICPOES are summarized in [Table 1](#).

Table 2. Certified reference materials and solder samples used in this work

Material ID	Use in project	Material	Bulk composition	Rosin core
SRM 1728	Calibration	Tin alloy	90:3:0.5 Sn:Cu:Ag	No
CRM 1131	Reference	Solder	40:60 Sn:Pb	No
C2416	Reference	Bullet lead	99% Pb	No
K2	Sample	Solder	Unknown	Yes
ON-003	Sample	Solder	60:40 Sn:Pb	Yes
EDM-3	Sample	Solder	Unknown	No
EDM-2	Sample	Solder	60:40 Sn:Pb	Yes
EDM-1	Sample	Solder	50:50 Sn:Pb	No
Dura-Pure 17657	Sample	Solder	50:50 Sn:Pb	No
Electrisol 17664	Sample	Solder	60:40 Sn:Pb	Yes
Oatey 48317	Sample	Solder	60:40 Sn:Pb	Yes

For tests of soldering iron temperature, a soldering iron and thermocouple were connected to a PL512 Mantle Minder Temperature Controller (GLAS-COL Apparatus Company, Terre Haute, USA). The thermocouple was contacted to the soldering tip to monitor iron temperature immediately preceding melting. Slight deviations in temperature are expected due to reported precision limits ($\pm 1.5\%$ of full scale)²¹ from the manufacturer.

The following analyte emission lines were monitored in samples: Ag I (328.068 nm), As I (189.042 nm), Bi I (223.061 nm), Cu I (324.754 nm), Fe I (373.486 nm), Pb II (172.680 nm), Sb I (217.581 nm), and Sn II (175.790 nm). These emission lines were selected based on maximum sensitivity and intensity, minimum spectroscopic interference, and day-to-day reproducibility.

Standard reference materials, gases, and samples. A variety of standard reference materials (SRMs) and commercially available solders were used in this project (Table 2). SRM 1728, a tin-alloy material, was used for matrix-matched external calibration. SRM C2416 and CRM 1131 were used for routine validation of the calibration and quality control. All SRMs in this research were obtained from the National Institute of Standards and Technology (NIST, Gaithersburg, MD, USA).

Pure argon (99.996%, MEGS Specialty Gases, Ottawa, ON, Canada) is used for all gas flows of the ICP, and for the carrier and bypass gases of the ETV assembly. Carbon tetrafluoride (MEGS Specialty Gases) reaction gas supplemented the carrier gas flow to increase analyte volatility and transport efficiency.

Melting procedures. Solder samples were melted by contacting the tip of the soldering iron with a solder sample only until solder wetting was visible, between 2–10 s, depending on the sample thickness and alloy melting point. Between melting different samples, the tip of the soldering iron was cleaned with 10% (v/v) HNO₃ (prepared through dilution of 68.0%–70.0% (assay) HNO₃ from Anachemia, VWR International LLC) then DDW purified to a resistivity of 18.2 M Ω cm (Arium Pro UV/DI, Sartorius Stedim Biotech, Göttingen, Germany).

When testing for the effect of sample size on contamination, solder samples Electrisol, Oatey, and Dura-Pure were cut into portions of 0.5 cm, 1.0 cm, 2.0 cm, and 3.0 cm. The temperature of the soldering iron was held at 350°C for these tests. When testing different soldering temperature conditions, solder samples Electrisol, Oatey, and Dura-Pure were cut into portions of 1 cm and melted at 200°C, 300°C, and 400°C. When testing for contamination between solder samples, 0.5-cm portions of solders Electrisol, Oatey, and Dura-Pure were melted in sequence with the temperature of the iron held at 350°C and without intermediate cleaning.

Analysis procedure. Solder sub-samples were cut into small chippings (approximately 1.5 mg) using a number 11 scalpel blade (Feather Safety Razor Co., Osaka, Japan). Five chippings of each sample were prepared for replicate measurements. External calibration curves were constructed using five chippings of SRM 1728, in weights ranging from 1.0 mg to 3.0 mg. Samples were loaded into individual graphite boats and introduced into the graphite furnace for a 100 s, 5-step analysis program (Table 1). Graphite boats were individually cleaned in the ETV furnace using a programmed cleaning cycle (Table 1). This was done preceding an analysis, and between analyses of different samples, to ensure the boats were clear of sample residue.

Data processing, internal standardization, and background correction. Transient signal profiles were collected for studied analytes and exported to Excel for processing. For each analyte signal, point-by-point internal standardization was done with the Ar I (404.442 nm) emission line. This technique compensates for sample loading effects on the plasma and instrument drift. Other Ar emission lines may be used for internal standardization in ETV-ICPOES; Ar I (415.859 nm),^{20,22} Ar I (763.511 nm),^{9,10,14} and Ar I (430.010 nm)¹² have been used in various applications. Ar I (404.442 nm) was selected for this research as it demonstrated day-to-day stability and the same signal suppression (an artefact of sample loading) among sample matrices.

A background correction technique was then applied to

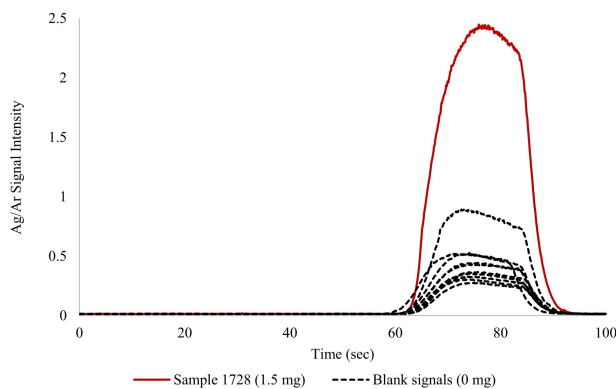


Fig. 1 Temporal profiles for Ag from 10 replicate blanks (empty graphite boats) and from a 1.5-mg sample of 1728, after point-by-point internal standardization with Ar 404.442 nm.

Fig. 2 Effect of blank subtraction and background correction on the integrated signal generated by 1.5-mg sample of 1728 relative to that observed without any correction.

eliminate the positive bias from background emission, as proposed by Maung and Beauchemin.²³ This replaces the blank subtraction method used conventionally with ETV-ICPOES where the average signal from 10 blank samples (*i.e.*, empty graphite boats) is subtracted from analyte profiles.^{5,10-14} Background correction instead takes the average signal before and/or after the analyte peak and subtracts this point-by-point from transient profiles; in this work, the signal immediately preceding vaporization (*e.g.*, time 0–50 s) was sufficient as the average background. To complete data processing, the peak area was integrated over the 30 s vaporization time step.

RESULTS AND DISCUSSION

Effect of background correction on analysis. Conventionally, the average blank signals from 10 empty graphite boats is used for

blank subtraction. In this work, background signals obtained during the analysis of calibration standards were taken in place of blank signals because great variability and even contamination often resulted during the analysis of empty graphite boats, as illustrated in Fig. 1. This affected the integrated signal, as shown in Fig. 2, where background correction systematically resulted in more analyte signal. The benefit of background correction versus blank subtraction is particularly striking for Fe, Pb and Sb. Background correction thus improves sample analysis in several ways: (1) increasing the total signal integration of analytes, and therefore improving LODs (not shown), (2) preventing negative signal integration in the case of trace determinations with high background or using contaminated graphite boats, and (3) decreasing analysis time by 10 analyses, which are otherwise required to generate an average blank signal ($n=10$).

Method validation. Four SRMs were analyzed routinely for validation of the calibration and analytical method. SRM 1131 and C2416 contained matrices highly similar to those of solder samples and enabled the validation of elements within the linear dynamic range. SRM 8437 and SRM 2710, both agricultural samples, were added exclusively to monitor Fe and Cr, respectively. These materials contain Fe and Cr concentrations that mirror those observed in solder and have established material homogeneity that is suitable for quality control in this research. All elements, with the exception of Cu and Pb, agree with the certified values. These exceptions are due to the large discrepancies in concentrations between the calibration SRM and the reference SRMs; for example, there is a 1102-fold difference of Cu concentration with SRM 1131, and a 47-fold difference of Pb with C2416. They were thus omitted from Table 3. The relative standard deviation (RSD) ranges from 11% (for Fe in SRM 8437) to 38% (for As in SRM 2710), which is typical of solid-sampling ETV analysis of mg aliquots.¹⁵ In fact, 1.5 mg is significantly less than the representative amount indicated on the certificates and thus reflects inhomogeneity of the materials at the mg level. However, this does not prevent accurate analysis down to 1 mg aliquots, as previously demonstrated by Becker,²⁴ and evident in Table 4. These RSDs are acceptable in exchange for a fast, simple, and convenient direct analysis method.

The method was also cross-verified by comparing most element concentrations for solder samples previously analyzed by inductively coupled plasma mass spectrometry (ICPMS) (Table 5). A Student's *t*-test at the 95% confidence interval indicates agreement for Sb, Bi and Sn ($p = 0.08-0.91$), thereby confirming the accuracy of the proposed analytical method. The disagreement for Cu and Pb was anticipated due to the aforementioned concentration discrepancies between standards and samples. This does not prevent qualitative analysis using these elements, as will be seen in the Alternative discrimination model section, which is even simpler. Hence, alternative calibration strategies to enable quantitative determination of these elements were not pursued.

Table 3. Average concentrations (%; mean ± standard deviation, n = 5) obtained for selected elements in SRMs. Elements with no reported values were either not certified or were beyond the linear dynamic range of calibration

SRM		As	Bi	Cr	Fe	Sb	Sn
1131	Measured	0.0094 ± 0.0011	0.0587 ± 0.0099	–	–	0.485 ± 0.076	44.9 ± 8.1
	Certified	0.01	0.06	–	–	0.43	39.3
C2416	Measured	0.065 ± 0.013	0.10 ± 0.03	–	–	0.83 ± 0.11	–
	Certified	0.056 ± 0.001	0.10 ± 0.01	–	–	0.79 ± 0.01	0.09 ± 0.01
8437	Measured	–	–	–	0.0040 ± 0.00045	–	–
	Certified	–	–	(0.0000026)	0.0031 ± 0.0006	–	–
2710	Measured	0.073 ± 0.028	–	0.0041 ± 0.0013	–	–	–
	Certified	0.0626 ± 0.0038	–	(0.0039)	3.38	0.0038 ± 0.0003	–

Table 4. Comparison of current ETV-ICPOES data (n = 5) to ICPMS data (n = 6) from Huang *et al.*³ for solder samples. Elements in agreement have concentrations that are not significantly different (at the 95% confidence interval) between ICPMS and ETV-ICPOES methods

Solder	Elements in agreement (p < 0.05)	Elements not in agreement (p ≥ 0.05)
EDM-3	Sb, Bi, Sn	Cu, Pb
K2	Sb, Bi, Sn	Cu, Pb
ON-003	Sb, Bi, Sn	Cu, Pb
EDM-1	Sb, Bi, Sn	Cu, Pb

etching of trace elements from the soldering iron tip during the melting process because of the additional time required to melt the larger area of solder, therefore increasing the contact time between the soldering tip and sample. To assess the significance of etching, element concentrations among four sample groups—unmelted solder (control), 0.5-cm solder melt, 1.0-cm solder melt, 2.5-cm solder melt, 3.0-cm solder melt—were compared (Fig. 3). A one-way analysis of variance (ANOVA) was used to assess if there was a significant change in element concentration after melting. This process was repeated for three types of solder. No significant statistical difference resulted among the groups for all solders tested (Table S1). Hence, etching does not vary with solder size.

Comparisons were additionally performed between the control group and a single melted experimental group. This would resolve possible etching that may occur in one specific size condition rather than another, which may not be isolated when examining differences holistically using an ANOVA test. Comparisons were done for each element using an unpaired Student’s t-test at the 95% confidence interval. The results for Dura-pure solder (Table S2) show that all elements agree between the unmelted portion and each melted size portion (p = 0.3–0.9). Similar results (not shown) were obtained for Electrisol and Oatey solders.

Effect of soldering temperature. The temperature of the soldering iron was varied to assess if temperature leads to significant change in element concentration. In previous work, soldering temperature was held constant at 350°C for all samples (with the exception of sample ON-003, which was melted at 300°C), which produced no significant change in concentration for elements Ag, As, Bi, Cu, Pb, Sb and Sn.⁸ In this study, three melting temperatures were tested to examine contamination from the Fe-tip soldering iron: 200°C, 300°C, and 400°C. The results are shown for three solders in Fig. 4. For each solder, an ANOVA test confirmed no significant difference among element concentrations between each test condition (Table S3). A Student’s t-test between control and individual test conditions (unmelted vs. 200°C, unmelted vs. 300°C, unmelted vs. 400°C) of solder Dura-Pure further confirmed no significance difference (p = 0.19–0.95) in element concentrations after melting between any two test

Fig. 3 Element concentrations (n = 5, except n = 3–5 for Fe and Cr in Electrisol) in unmelted and melted portions of various sizes of solders Dura-Pure (top), Oatey (middle) and Electrisol (bottom).

Effect of solder size. An increased length of solder may facilitate

Table 5. Blind test for identification of unknown solder (Dura-pure 17657) using mass-corrected element signals that were integrated and computed as a range (mean \pm 1 standard deviation) for comparison; T = match (*i.e.*, element range overlaps), F = no match (*i.e.*, = element ranges do not overlap). A sample is identified when all ranges overlap

	Unknown solder (Dura-pure 17657)								
	Ag	As	Bi	Cr	Cu	Fe	Pb	Sb	Sn
CRM 1131	F	F	F	F	F	F	F	F	F
K2	T	F	F	F	F	F	F	F	T
ON-003	F	F	F	F	F	F	F	F	T
EDM-1	F	F	F	F	F	F	T	F	T
EDM-2	F	F	F	F	F	F	T	F	T
EDM-3	F	F	F	F	F	F	T	F	F
Dura-Pure 17657	T	T	T	T	T	T	T	T	T
Electrisol 17664	T	T	F	T	F	T	T	T	T
Oatey 48317	F	T	F	T	T	T	T	T	T

the case of rosin-core solders, which have been shown to leach trace metals due to their acidity,^{2,3,5} etching from the Fe-tip soldering gun did not measurably occur.

Contamination between soldering samples. One final possibility for etching is between solder samples as they are melted in series, with no cleaning intervention. Past solder research has involved some frequent cleaning of the soldering tip, which may directly etch the surface of the tip to prevent contamination to a sample, or perhaps remove deposit leftover from melting solder, thus preventing cross-contamination between one solder to another. To test if contamination by either mean is persistent, three solders, Electrisol, Oatey, and Dura-Pure, were melted in sequence without cleaning the soldering tip.

If contamination did occur from a lack of cleaning, it would be evident in either Oatey or Electrisol, which were melted later in the sequence. However, a Student's t-test at the 95% confidence interval (Table S5) confirmed no significant change in concentration between unmelted and melted fractions, even for the latter two solders ($p = 0.06-0.61$). This provides evidence that no significant cross-contamination occurs when melting different solders in series without a cleaning step. Furthermore, a melted solder (Dura-Pure) from a clean tip produced an average relative standard deviation (RSD) of $19.8 \pm 4.9\%$ compared to an average RSD of $15.4 \pm 8.1\%$ when the same sample was melted with an uncleaned tip. Expectedly, an F-test confirmed no significant difference in precision when a sample was melted with either tip (F values ranging from 1.34–2.92, $F_{crit} = 4.11$). In future work, no cleaning of the soldering tip is necessary when studying the soldering procedure, which will decrease analysis time and remove the need to obtain acid or acidic solutions.

Alternative discrimination model. In past research, the discrimination of solder has been achieved using a model developed by Suzuki *et al.*,² which compares trace and major element concentrations among solders. This model assigns each element concentration as a range (mean \pm 2 standard deviations), and ranges that overlap are tabulated as a match. When the ranges

Fig. 4 Element concentrations ($n = 5$) in solders Dura-Pure (top), Oatey (middle) and Electrisol (bottom) that were melted at various temperatures or unmelted.

conditions (Table S4). This result is consistent among solders Electrisol and Oatey (not shown).

The lack of significant contamination after melting may be due to the increased corrosion resistance of the Fe-based soldering tip. The Fe-plated tip used in this research, and in many other Fe or stainless-steel soldering tips, contains an appreciable fraction of Cr (between 12 to 30%, depending on the grade)²⁵ to allow the formation of a Cr-rich surface oxide film. This film behaves as a shield against corrosion,⁷ and may be a factor for why the solder does not leach any of the trace and major elements tested. Even in

of all elements match, solders are considered to be the same. This has been harnessed to correctly match a melted sample with its unmelted pair amongst a bank of various lead-tin solders.⁵ Both works demonstrate the need for only 3 elements for successful discrimination.

Though this technique by Suzuki *et al.* is effective, it requires the construction of an external calibration curve for each monitored element and complete quantitative interpolation of a dataset. In this work, a new procedure focused solely on qualitative elemental data is proposed. To this end, one sample of solder was randomly selected from a bank of 8 solder materials and assigned as the test unknown. Five replicates of each sample, including the unknown sample, were measured. Instead of computing element concentrations, element peak areas were integrated and mass-corrected. The average of five replicates provided a range (mean \pm 1 standard deviation) for element-by-element comparison. The results of this blind test are compiled in Table 5. As shown, there is only one sample for which all element ranges match with the unknown; this confirms that the unknown was correctly and discretely identified as Dura-Pure 17657. As no calibration was required, analytes Pb II (172.680 nm) and Cu I (324.754 nm) could be incorporated into the analysis. Impressively, most elements alone could achieve discrimination of two-thirds of solders within the sample bank (6 out of 9 samples). The element with the least amount of discrimination power was Pb, which excluded 3/9 solders in the blind trial. Though only one element (Bi) was sufficient to discriminate all but the unknown in this limited solder bank, at a minimum, 2–3 elements should be used in the discrimination model.

CONCLUSION

This study determined trace and major elements of solder when melting under varying user conditions of sample size and temperature. Melting solder of different sizes (0.5–3 cm) or increasing the temperature of the soldering iron caused no significant change in concentrations after melting. These observations are consistent for solders with or without rosin, and indicate the absence of significant etching of the major tip elements when using a Fe-tip soldering iron. This is in contrast to melting rosin-containing solders using a Cu-tip soldering iron, which etched Cu.^{3,5}

Present research observations provide additional context for solder contamination, which adds to the knowledge-base for the forensic analysis of solders. The background correction technique eases the procedure for analyzing trace alloyed materials or other forensic evidence by replacing blank subtraction, which also improves LODs and decreases overall analysis time. Eliminating solder-tip cleaning better aligns with how IEDs are realistically

produced. Qualitative discrimination using mass-corrected peak areas is a simpler and faster approach for solder discrimination and may be suitable as an alternative to conventional quantitative strategies to understand and anticipate how a salvaged solder sample can be properly paired with its reference, and how changes (or lack thereof) in concentration implicate specific soldering tools (on the basis of soldering tip material). Most importantly, there is added assurance that these predictions are robust despite inherent user variations in soldering conditions, such as soldering temperature or solder size. The use of ETV-ICPOES is a promising analytical technique for the discrimination of solders, and including elements like Fe and Cr makes this approach suitable for the analysis of stainless steels or other ferrous-alloys. It can thus be applied to a variety of crime-related devices (*e.g.*, tools, weapons, cordage, etc.) as well as other artefacts and fragments (*e.g.*, debris, geological materials or soils, automobile parts).

In the future, multivariate statistical analyses such as linear discriminant analysis (LDA) and/or principal component analysis (PCA) will be explored to aid in discriminating solders and identify which variables affect discrimination most based on simple, visual classifications. These techniques have been applied in past forensic research (hair analysis,^{12,26} automotive paint analysis^{9,10}) to achieve high discrimination, and in some cases, up to 100% probability or prediction success.¹⁰ This would facilitate solder analysis as some methods of multivariate analysis (*e.g.*, LDA) do not require quantitative analysis, but instead rely on peak integration.

ASSOCIATED CONTENT

The supporting information (Tables S1–S5) is available at www.at-spectrosc.com/as/home

AUTHOR INFORMATION



Diane Beauchemin received her Ph.D. in 1984 from Université de Montréal. She is a professor (Full) at Queen's University. Her research efforts are focused on inductively coupled plasma mass spectrometry (ICPMS) and ICP optical emission spectrometry (OES) from both fundamental and application perspectives, and expanding the range of application of ICPMS/OES to geochemical exploration, risk assessment of food safety, characterization of nanoparticles, and forensic analysis. She has been working as member of editorial board for *Atomic Spectroscopy*. Diane Beauchemin won the Alan Date Memorial Award (1988) from VG

Elemental, the Distinguished Service Award (2001) from Spectroscopy Society of Canada, the Maxxam Award (2017) and Clara Benson Award (2019) from Canadian Society for Chemistry, and the Gerhard Herzberg Award (2018) from the Canadian Society for Analytical Sciences and Spectroscopy. She is author or co-author of over 160 articles published in peer-reviewed scientific journals.

Corresponding Author

*D. Beauchemin

Email address: diane.beauchemin@queensu.ca

Notes

The authors have no conflicts to declare.

ACKNOWLEDGMENTS

The authors gratefully acknowledge the financial support of the Natural Sciences and Engineering Research Council of Canada (RGPNM 39487-2018). KM and CW are grateful to Queen's University School of Graduate Studies for graduate awards.

REFERENCES

1. National Academies and the Department of Homeland Security, *IED Attack: Improvised Explosive Devices*. https://www.dhs.gov/sites/default/files/publications/prep_ied_fact_sheet.pdf
2. Y. Suzuki, M. Kasamatsu, S. Suzuki, and Y. Marumo. *Anal. Sci.*, 2003, **19**, 415–418. <https://doi.org/10.2116/analsci.19.415>
3. L. Huang, D. Beauchemin, and C. Dalpé, *J. Anal. At. Spectrom.*, 2018, **33**, 1784–1789. <https://doi.org/10.1039/C8JA00222C>
4. J. W. Evans, *A Guide to Lead-free Solders*, Springer International Publishing, London, England, 2007. <https://link.springer.com/book/10.1007/978-1-84628-310-9>
5. M. MacConnachie, K. Moghadam, and D. Beauchemin, *J. Anal. At. Spectrom.*, 2021, **36**, 1600–1606. <https://doi.org/10.1039/D1JA00172H>
6. OK International, *Technical Note v. 2.2.*, Newark, NJ, 2007. <https://www.okinternational.com/home/>
7. C. Stuber, *How to Maximize Soldering Iron Tip Life*, HakkoUSA Knowledge Base, 2021. <http://kb.hakkousa.com/Knowledgebase/10322/How-to-Maximize-Soldering-Iron-Tip-Life>
8. P. Walker and W. H Tarn, *Handbook of Metal Etchants*, CRC Press, London, England, 1991. <https://doi.org/10.1201/9781439822531>
9. A. Asfaw, G. Wibetoe, and D. Beauchemin, *J. Anal. At. Spectrom.*, 2023, **27**, 1928–1934. <https://doi.org/10.1039/C2JA30193H>
10. L. Huang and D. Beauchemin, *J. Anal. At. Spectrom.*, 2017, **32**, 1601–1607. <https://doi.org/10.1039/C7JA00196G>
11. M. MacConnachie, M. Lapointe, E. Galiano, and D. Beauchemin, *J. Anal. At. Spectrom.*, 2020, **35**, 2487–2493. <https://doi.org/10.1039/D0JA00288G>
12. M. MacConnachie, S. Lu, Y. Wang, J. Williams, and D. Beauchemin, *RSC Adv.*, 2022, **12**, 27064–27071. <https://doi.org/10.1039/D2RA05654B>
13. A-S. Masquelin, F. Kaveh, A. Asfaw, C. J. Oates, and D. Beauchemin, *Geochem.: Explor. Environ. Anal.*, 2013, **13**, 11–20. <https://doi.org/10.1144/geochem2012-129>
14. A. A. Hejami and D. Beauchemin, *J. Anal. At. Spectrom.*, 2019, **34**, 1426–1432. <https://doi.org/10.1039/C8JA00266E>
15. F. Kaveh, C. J. Oates, and D. Beauchemin, *Geochem. Explor. Environ. Anal.*, 2014, **14**, 305–313. <https://doi.org/10.1144/geochem2013-230>
16. F. Kaveh and D. Beauchemin, *J. Anal. At. Spectrom.*, 2014, **29**, 1371–1377. <https://doi.org/10.1039/C4JA00041B>
17. N. Sadiq and D. Beauchemin, *Anal. Chim. Acta*, 2014, **851**, 23–29. <http://doi.org/10.1016/j.aca.2014.09.017>
18. R. A. Althobiti and D. Beauchemin, *J. Anal. At. Spectrom.*, 2021, **36**, 535–539. <https://doi.org/10.1039/D0JA00479K>
19. D. C. Harris, *Br. Med. J.*, 2010, **2**, 908–909. [http://doi.org/10.1016/0021-9673\(91\)85187-K](http://doi.org/10.1016/0021-9673(91)85187-K)
20. G. L. Scheffler, A. J. Brooks, Z. Yao, M. R. Daymond, D. Pozebon, and D. Beauchemin, *J. Anal. At. Spectrom.*, 2016, **31**, 2434–2440. <https://doi.org/10.1039/C6JA00369A>
21. VWR International. <https://ca.vwr.com/store/product/en/4563183/mantle-mindertm-ii-automatic-temperature-controller-glas-col>
22. K. Harrington, A. A. Hejami, and D. Beauchemin, *J. Anal. At. Spectrom.*, 2020, **35**, 461–466. <https://doi.org/10.1039/C9JA00400A>
23. P. Maung and D. Beauchemin, *J. Anal. At. Spectrom.*, 2021, **36**, 1104–1111. <https://doi.org/10.1039/D1JA00090J>
24. J. S. Becker, *Can. J. Anal. Sci. Spectrosc.*, 2002, **47**, 98–108. <https://doi.org/10.1056/NEJM199407283310407>
25. R. P. Singh, S. E. Zorrilla, S. K. Vidyarthi, R. Cocker, and K. Cronin, *Ency. D. Sci.*, 2022, 239–252. <https://doi.org/10.1016/B978-0-12-818766-1.00197-5>
26. L. Huang and D. Beauchemin, *J. Anal. At. Spectrom.*, 2014, **29**, 1228–1232. <https://doi.org/10.1039/C4JA00071D>